Focal properties of laser driven micro-lens to focus and energy select MeV protons

T. Toncian, M. Amin, R. Jung, A. C. Pipahl and O. Willi
Institut für Laser und Plasma Physik, Heinrich-Heine-Universität, Düsseldorf, Universitätstrasse 1, 40225 Düsseldorf, Germany

M. Borghesi, C. A. Cechetti and P. A. Wilson
School of Mathematics and Physics, The Queen's University, Belfast, UK

J. Fuchs
Laboratoire pour l'Utilisation des Lasers Intenses, UMR 7605 CNRS-CEA-École Polytechnique-Université Paris VI, Palaiseau, France

R. J. Clarke and M. M. Notley
Central Laser Facility, STFC, Rutherford Appleton Laboratory, Chilton, Didcot, Oxfordshire, OX11 0QX, UK

Main contact email address **toncian@uni-duesseldorf.de**

Introduction

The recent development of ultra-intense laser pulses [1] has opened up opportunities for applications in many areas including particle acceleration [2-5] inertial fusion energy [6], generation of intense x-ray pulses [7], laser-driven nuclear physics [8] and laboratory astrophysics [9]. In particular, the acceleration of MeV ions from the interaction of high-intensity laser-pulses with thin solid targets has major applicative prospects due to the high beam quality of these ion bursts [10, 11]. Such proton beams are already applied to produce high energy density matter [12] or to radiograph transient processes [13], and offer high prospects for tumour therapy [14], isotope generation for positron emission tomography [15], fast ignition of fusion cores [16], and brightness increase of conventional accelerators. However, as these proton beams are poly-energetic and divergent at source, reduction and control of their divergence and energy spread are essential requirements for most of these applications. Focussing and energy selection of part of such poly-energetic and divergent proton beams have been demonstrated [17]. Here we investigate the properties of the focal length for different proton energies.

Experimetal Setup

The experiment was conducted at Target Area West at the RAL Laboratory, employing the Vulcan laser [18] operating in the Chirped Pulse Amplification mode (CPA). The two arms CPA1 and CPA2 of the Vulcan laser were compressed to 1.2 ps. The pulse length was monitored by a second order online autocorrelator under full energy shot condition. The delay between the two pulses was controlled optically with picosecond precision. The laser pulses were focused by F/3.2 parabolas (60 cm focal length) to a 11 µm FWHM focal spot. The CPA1 pulse (irradiance $I=8\times10^{18}$ W/cm^2) was used to accelerate a high-current, diverging beam of up to 18 MeV protons from a 25 µm thick Au foil target (the protons are produced from hydrocarbon impurities [18] on the target rear surface [20,21]). The CPA2 pulse ($I=8\times10^{18}$ W/cm^2) was focused onto the outer wall of a hollow cylinder. The proton beam from the first foil was directed through the cylinder and detected with a stack of Radiochromic Films (RCF, a dosimetric detector [22]) positioned at a variable (from 5 to 10 cm) distance from the proton source. The RCF stack was used to measure the proton beam divergence. It also provided a coarse energy resolution due to the energy deposition properties of the ions [3] (most of the energy of a proton is released in the so-called Bragg peak, located at a distance in the detector which depends on the incident proton energy). It was shielded with an 11 µm Al foil allowing protons with energies above 1.1 MeV to be recorded. In some cases, a central mm-sized hole was bored through the RCF to allow downstream high spectral resolution measurements using a magnetic spectrometer with a 0.6 T permanent magnet. The spectral resolution determined by the slit width and the dispersion of the spectrometer is 0.2 MeV at 6 MeV and 0.7 MeV at 15 MeV.

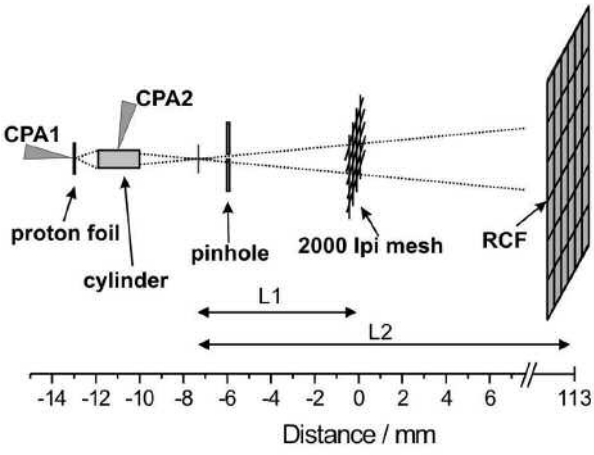

Figure 1. Experimental setup.

The experimental setup is shown in fig. 1. The distance from the Au proton production foil and the cylinder entrance was 1 mm. The cylinder material was Dural (95% Al, 4% Cu, 1% Mg) with a length of 2 mm and an outer diameter of 810 µm. The wall thickness was 50 µm and the cylinder was held by a 100 µm tungsten wire. In order to investigate the energy dependent divergence of the proton beam altered by the micro lens, we placed a thin Cu mesh with 2000 lpi 10 mm after the exit of the cylinder. Protons with different energies will transit through the cylinder at different times and will be influenced by the different evolution stages of the electric field inside micro-lens. Since the protons will leave with different divergences the RCF will record different magnified images of the mesh. For sufficient magnification on the detector plane the RCF had to be positioned ~10 cm from the cylinder exit. At this distance the proton beam was very diluted and to

maximize the contrast of the measurement we subapertured the proton beam with a 200 µm pinhole placed at 4.5 mm behind the cylinder exit. The projected mesh created by high energy protons and electrons that were not affected by the not yet triggered micro-lens can be seen in fig. 2 (0-order). Knowing that the distance between proton foil and mesh was set with tens of µm precision the 0-oder mesh geometric magnification defines the plane of the RCF detector. In the case of result shown in figure 2D a distance of 100.3 mm was used. The magnification in this case was 8.9 fold.

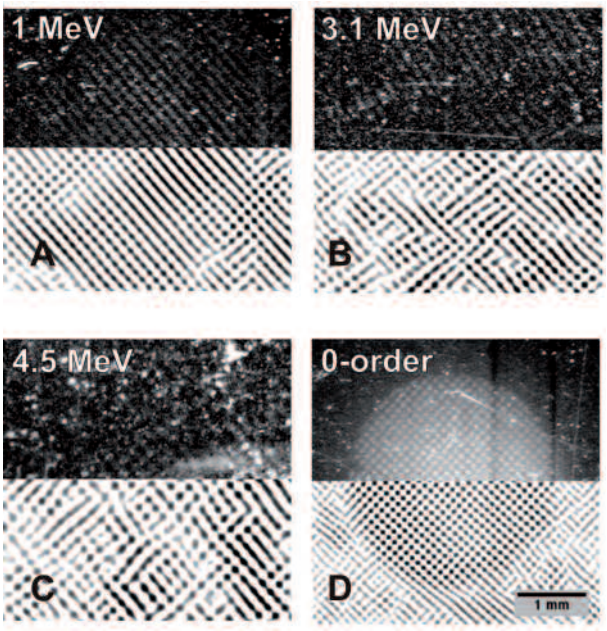

Figure 2. Divergence reconstruction data, top part show raw dose deposition on RCF, bottom part shows enhanced mesh image after Fourier filtering.

Results

The optical time delay between CPA1 and CPA2 was set so that a quasi-monoenergetic peak at 7 MeV could be measured in the magnetic spectrometer. These protons almost exiting the lens when this is triggered feel the focusing fields just for a short time and are just collimated by the micro-lens. Thus their matched divergence to the spectrometer entrance slit will result in an increase of the measured flux. Protons that are focused in between the cylinder exit and the mesh will project a magnified mesh on the detector plane. Figure 2A-C top parts show the mesh projection by protons with energies of 1 MeV, 3.15 MeV and 4.4 MeV, respectively. To extract the periodicity of the magnified mesh the data has been contrast enhanced and the first order of the 2D Fourier transform has been considered. From figure 2A-C a magnification of M=11.4, 12.2, 14.8 has been computed for the 1 MeV, 3.15 MeV and 4.4 MeV protons respectively. Simple geometrical ray tracing yields the focal lengths of 0.4 mm, 1 mm and 2.7 mm from the exit of the cylinder for the three energies mentioned above. By reducing the pulse energy and thus also the intensity by 20 % the focal lengths (again in respect to the exit of the cylinder) were 0.9 mm for 1 MeV, 2.8 mm for 3.15 MeV, and 4.7 mm for 4.4 MeV protons.

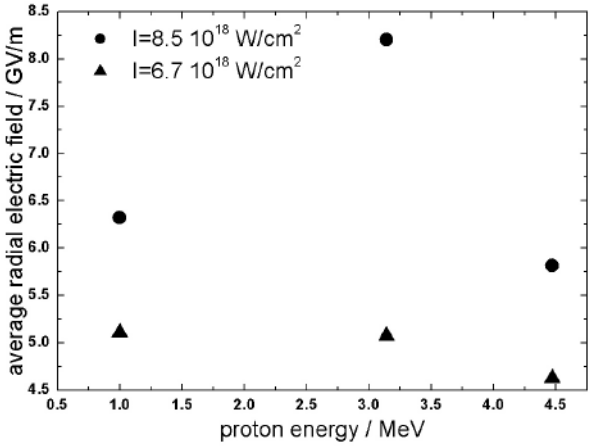

Figure 3. Estimated average electric field.

A time integrated average radial electric field can be estimated. Let us consider that the protons begin to be deflected as soon as the lens has been triggered and they will be deflected up to the time they exit the cylinder or the field has collapsed. From measurements that are to be presented in another publication we infer that the time evolution of the field is peaked around 20 ps, collapses between 20 and 60 ps after triggering. It spreads over the cylinder surface with ~ 0.3 time the speed of light. Taking into account the optical delay between CPA1 and CPA2 the time of flight of the protons and field evolution history we reconstruct following scenario. The 4.5 MeV protons are around 80 µm in front of the exit of the cylinder when the lens is triggered. In other words having a transit time of 15 ps these protons will be deflected by the rising edge of the field and they will exit the cylinder before the maximal field strength is reached. The 3.15 MeV protons are inside the cylinder during the whole of the interaction. These protons will be focused with the shortest focal length. The 1 MeV protons are outside the cylinder when the fields are triggered. They will reach the focusing fields just when these are collapsing, therefore being less deflected. The time averaged field strengths are given in fig 3. The measured field strengths are found to be in the order several of GV/m.

In conclusion we have measured the focal proprieties of the laser triggered micro lens for the first time. The lens showed a chromatic behaviour that can be exploited to energy select from a broad band beam. Measurements show that by tuning the intensity of the field triggering laser the focal length of the lens can be tuned.

We acknowledge the expert support from the technical teams at RAL. This work has been supported by EU-Grant No. HPRICT 1999-0052, and DFG SFB TR18 and GRK 1203, and partly by the QUB-IRCEP scheme.

References

1. M. D. Perry and G. Mourou, *Science* **264**, 917 (1994).
2. E. Clark *et al.*, *Phys. Rev. Lett.* **84**, 670 (2000).
3. R. Snavely *et. al.*, *Phys. Rev. Lett.* **85**, 2945 (2000).
4. A. Maksimchuk *et al.*, *Phys. Rev. Lett.* **84**, 4108 (2000).
5. V. Malka *et al.*, *Plasma Phys. Control. Fusion* **47**, B481 (2005) and references within.

6. M. Tabak *et al*., *Phys. Plasmas* **1**, 1626 (1994).
7. A. Rousse *et al*., *Phys. Rev. Lett.* **93**, 135005/1 (2004).
8. K.W. D. Ledingham, P. McKenna and R. P. Shinghal, *Science* **300**, 1107 (2003).
9. B. A. Remington, D. Arnet, R. P. Drake and H. Takabe, *Science* **284**, 1488 (1999).
10. M. Borghesi *et al*., *Phys. Rev. Lett.* **92**, 055003/1 (2004).
11. T. Cowan *et al.*, *Phys. Rev. Lett*. **92**, 204801/1 (2004).
12. P. Patel *et al*., *Phys. Rev. Lett.* **91**, 125004/1 (2003).
13. M. Borghesi *et al*., *Phys. Plasmas* **9**, 2214 (2002).
14. S.V. Bulanov *et al*., *Phys. Lett. A* **299**, 240 (2002).
15. I. Spencer *et al.*, *Nucl. Inst. And Meth. In Phys. Research B* **183**, 449 (2001).
16. M. Roth *et al*., *Phys. Rev. Lett.* **86**, 436 (2001).
17. T. Toncian *et al*., *Science* **312**, 410 (2006), Willi O. *et al*., *Laser Part. Beams* **25**, 71 (2007).
18. C. N. Danson *et al.*, *Laser and Part. Beams* **17**, 341 (1999).
19. M. Hegelich *et al*., *Phys. Rev. Lett.* **89**, 085002/1 (2002).
20. S.C. Wilks *et al*., *Phys. Plasmas* **8**, 542 (2001).
21. L. Romagnani *et al*., *Phys. Rev. Lett.* **95**, 195001/1 (2005).
22. GAFCHROMIC Radiochromic Dosimetry Films, www.ispcorp.com